Cell Stem Cell, volume 9

Supplemental Information

Nodal/Activin Signaling Drives Self-Renewal and Tumorigenicity of Pancreatic Cancer Stem Cells and Provides a Target for Combined Drug Therapy

Enza Lonardo, Patrick C. Hermann, Maria-Theresa Mueller, Stephan Huber, Anamaria Balic, Irene Miranda-Lorenzo, Sladjana Zagorac, Sonia Alcala, Iker Rodriguez-Arabaolaza, Juan Carlos Ramirez, Raul Torres-Ruíz, Elena Garcia, Manuel Hidalgo, David Álvaro Cebrián, Rainer Heuchel, Matthias Löhr, Frank Berger, Peter Bartenstein, Alexandra Aicher, and Christopher Heeschen

LEGENDS OF SUPLEMENTAL FIGURES

Supplementary Figure 1 (related to Figure 2): **Components of the Nodal signaling pathway are overexpressed in pancreatic CSC.** (**A**) Tumor take rate for cells isolated by flow cytometry using the surface markers CD44 and CD133 in A6L (left panel) and 185 (right panel) tumors. (**B**) Surface expression of Cripto, Alk4, and Alk5 in adherent (monolayer) versus sphere-derived (spheres) cells as assessed by flow cytometry. (**C**) QPCR analysis of TGF-β signaling-associated genes in adherent cells versus spheres. Data are normalized to *Gapdh* expression and are presented as fold change in gene expression relative to adherent cells. Data are mean ± SD, n≥3. (**D**) QPCR analysis of Nodal signaling-associated genes in adherent cells versus spheres in established pancreatic cancer cell lines L3.6pl and MiaPaCa. Data are normalized to *Gapdh* expression and are presented as fold change in gene expression relative to adherent cells. Data are mean ±SD, n≥3. (**E**) Western blot analysis for Nodal, Smad4, pSmad2 and Smad2/3 proteins in adherent cells versus spheres for the same cell lines. Parallel GAPDH immunoblotting was performed. (**F**) QPCR analysis of pluripotency-associated genes in adherent cells versus spheres for MCF7 breast cancer cells. Data are normalized to *Gapdh* expression and are presented as fold change in gene expression relative to adherent cells. Data are mean ±SD, n≥3. (**G**) QPCR analysis

of Nodal signaling–associated genes in adherent cells versus spheres for MCF7 breast cancer cells. Data are normalized to *Gapdh* expression and are presented as fold change in gene expression relative to controls (C=adherent cells). Data are mean ±SD, n≥3.

Supplementary Figure 2 (related to Figure 4): Colony formation assays in soft agar using 185 and A6L cells. Cells were seeded at a density of 4×10^3 cells per 35-mm dish and cultured in 0.35 % soft agar in RPMI containing 10% FBS at 37 °C for 14 days. Nodal recombinant protein (300 ng/ml) was added to the soft agar every two days. The colonies were stained with 0.05 % crystal violet. Colony numbers in the entire dish were counted. The average colony size was determined by measuring the diameters of colonies in 10 microscope fields with a microcaliper and dichotomized according to size.

Supplementary Figure 3 (related to Figure 5): Lentivirally transduced cell cultures were FACSorted to highest purity based on GFP expression (representative images of sorted cells are given in 1st panel). Comparison of *Alk4* mRNA expression levels (2nd panel), Alk4 surface expression assessed by flow cytometry (3rd panel), population doubling time (4th panel) after lentiviral delivery of scrambled or *Alk4* shRNA.

(**B**) Lentivirally transduced cell cultures were FACSorted to highest purity based on GFP expression (representative images of sorted cells are given in 1st panel). Comparison of *Alk5* mRNA expression levels (2nd panel), Alk5 surface expression assessed by flow cytometry (3rd panel), population doubling time (4th panel) after lentiviral delivery of scrambled or *Alk5* shRNA.

(**C**) Lentivirally transduced cell cultures were FACSorted to highest purity based on GFP expression (representative images of sorted cells are given in 1st panel). Comparison of *Nodal* and *Activin* mRNA expression levels (2nd panel), Nodal protein expression levels by western blot (3rd panel panel), population doubling time (4th panel, left), and proliferation index assessed by Ki67 staining (4th panel, right) after lentiviral delivery of *scrambled* or *Nodal* shRNA.

(**D**) Lentivirally transduced cell cultures were selected using puromycin resistance. Comparison of mRNA expression levels (1st panel), protein expression levels by western blot (2nd panel panel), and population doubling time (3rd panel, left) after lentiviral delivery of scrambled or *Smad4* shRNA.

Supplementary Figure 4 (related to Figure 5): (**A**) QPCR analysis of Nodal signaling–associated genes in A6L cells versus pancreatic stellate cells (PSC). Data are normalized for *Gapdh* expression and are mean ±SD, n≥3. For illustrative purposes, characteristics of the cells are displayed in the lower panel (Jesnowski R et al. Lab Invest 2005). (**B**) Invasion of sphere-derived cells in the presence or absence of conditioned medium from PSC in the lower compartment of Matrigel™-coated Boyden chambers. For preparation of PSC-conditioned medium, PSC were grown to 80% confluency in full medium (RPMI containing 10% FBS and antibiotics), which was then replaced by RPMI medium containing only 1% FBS and cultured for another 72 hours. (**C**) Sphere formation capacity of 185, A6L, and 354 cells in the presence of PSC-conditioned DMEM/F12 medium or control medium in ultralow adhesion 24-well plates.

Supplementary Figure 5 (related to Figure 6): ***In vivo* tumorigenicity of pretreated cells. (A)** Experimental setup for *in vivo* validation of tumorigenicity of pretreated L3.6pl cells. (**B**) Tumor take-rate (**upper left panel**), representative PET imaging (**upper right panel**), representative macroscopic pictures of the pancreata (**middle right panel**), and representative macroscopic pictures of livers (arrows indicate metastases; **lower right panel**) after orthotopical implantation of pretreated pancreatic cancer cells. (**C**) Flow cytometry for CD133 and CXCR4 in L3.6pl cells untreated or treated with Gemcitabine (GEM) alone or in combination with SB431542. (**D**) Flow cytometry for CD133 in L3.6pl cells treated with SB431542 alone (upper row) or together with Gemcitabine (GEM) (lower row). Analyses were performed at the end of treatment, 24 hours after withdrawal of treatment, and 48 hours after withdrawal of treatment. (**E**) Cell cycle analysis

of CD133 positive cells untreated, treated with SB431542, or treated with SB431542 plus GEM after 2 hours of pulsing with BrdU. R4 represents cells in S phase, R2 represents apoptotic cells.

Supplementary Figure 6 (related to Figure 7): ***In vivo*** **effects of Nodal/Activin inhibition on established primary pancreatic cancer xenografts.** (**A**) Tumor size of treated pancreatic cancers was measured on day 27 after initiation of treatment and is depicted as box and whisker plots indicating median and 25th and 75th percentiles as boxes and 5th and 95th percentiles as whiskers. (**B**) For target validation, tumors were explanted and expression of key pathway members was assessed by Western blotting, (**C**) QPCR, and **(D**) immunohistochemistry, comparing the two different treatment regimens. (**E**) Quantification of SB431542 in tumor samples was carried out using an Agilent 1200 HPLC (Agilent Technologies, Palo Alto; CA) system attached to an API2000 triple quadruple mass spectrometer (Applied Biosystems). Solvents used were miliQ water-0.1% formic acid (A) and acetonitrile-0.1% formic acid (B), and a gradient from 5% B to 100 % B was applied during 2.5 minutes with additional 1.5 minutes at 100% B for cleaning purposes. Quadruples were operated with unit resolution in the positive ion mode. The resulting multiple reaction monitoring (MRM) chromatograms were use for quantification by means of the Analyst software version 1.4 (MDS Sciex). Ion transitions chosen for detection of SB431542 were 385.200→181.200; 385.200→180.300; 385.200→208.800. Source and compound dependent parameters were automatically optimized for SB431542 allowing its specific detection.

Tumor samples were processed for analysis by homogenization in 3 volumes of miliQ water using mechanical homogenizer (Glas-col®). Homogenates were submitted to and ultrasound bath for 5 minutes and then centrifuged at 2500 g for 5 minutes. The supernatant was further processed by solid phase extraction using HybridSPE-protein precipitation (HybridSPE-PPT, Sigma Aldrich). Thus the proteins and phospholipids were depleted and the solution was submitted for LC-MS/MS analysis.

Calibration standards were prepared in a range from 20 ng/g tissue to 5 µg/g tissue by diluting 5 µL of methanol working solutions of SB431542 (Sigma-Aldrich) at different concentrations in 45 µL of homogenate from non-treated animals tumor samples. Quality control samples (QC) at 2 concentration levels (20 ng/g tissue and 5 µg/g tissue) were prepared in a similar way. A lower limit of quantification (LLOQ) of 20 ng/g tissue was achieved. The upper limit of quantification (ULOQ) was 5 g/g tissue. A compound from the Experimental Therapeutics Program (CNIO) was used as internal standard. Tumor samples from animals receiving allocated treatments were processed in the same way.

Supplementary Figure 7 (related to Figure 7): ***In vivo*** **effects of Nodal/Activin inhibition on established primary pancreatic cancer xenografts.** (**A**) Explanted primary pancreatic xenografts from **figure 7 D-G** treated with gemcitabine (GEM) alone or in combination with SB431542 (SB) or in combination with SB and the hedgehog pathway inhibitor CUR199691 (CUR) (n=12 per group). **(B)** Treatment of Smad4-mutated JH051 tumors with GEM alone or in combination with SB and CUR (n=8-10 per group).

Supplementary table 1: List of utilized primers

Gene	Primer sense	Primer antisense
Nanog	tgaacctcagctacaaacaggtg	aactgcatgcaggactgcagag
Oct3/4	cttgctgcagaagtgggtggaggaa	ctgcagtgtgggtttcgggca
Stat3	aaaactctcacggacgagga	gctgcaactcctccagtttc
Klf4	acccacacaggtgagaaacc	atgtgtaaggcgaggtggtc
Sox2	agaaccccaagatgcacaac	cggggccggtatttataatc
Nodal	agcatggttttggaggtgac	cctgcgagaggttggagtag
Cripto-1	tccttctacggacggaactg	atcacagccgggtagaaatg
FoxH1	ccccctaagaggaggaagaa	cttccctgaagaaggggaac
Smad2	cgaaatgccacggtagaaat	ccagaagagcagcaaattcc
Smad4	ccatttccaatcatcctgct	acctttgcctatgtgcaacc
Gdf1	actactgccagggtcagtgc	acgttgtcgctgttgtcaaa
Activin	aaagcttcatgtgggcaaag	aatctcgaagtgcagcgtct
Alk4	ggagcgtcttgtctttggag	tgcaacaggatcgacttgag
Cripto-3	gtgatttggatcatggccatttctaaagc	gctgtcatctctgaaggccaggtc
Gapdh	caggagcgagatccct	ggtgctaagcagttggt
Tgfb1	aagtggacatcaacgggttc	tgcggaagtcaatgtacagc
Alk5	gatgggctctgctttgtctc	caaggccaggtgatgacttt
TgfbRII	ggggaaacaatactggctga	gagctcttgaggtccctgtg
Lgr5	cggaggaagcgctacagaat	ctgggtggcacgtagctgat
CXCR4	ggtggtctatgttggcgtct	tggagtgtgacagcttggag

Supplementary table 2: List of utilized shRNA

ShNodal
ID: TRCN0000058699
> shNODAL Sense
gatccGCGGTTTCAGATGGACCTATTCTCGAGAATAGGTCCATCTGAAACCGCTTTTTTg
> shNODAL Antisense
aattcAAAAAAGCGGTTTCAGATGGACCTATTCTCGAGAATAGGTCCATCTGAAACCGCg

ShALK4
ID: TRCN0000001812
>shALK4_3 Sense
gatccAGCAGAGATATACCAGACGGTCTCGAGACCGTCTGGTATATCTCTGCTTTTTTTg
>shALK4_3 Antisense
aattcAAAAAAAGCAGAGATATACCAGACGGTCTCGAGACCGTCTGGTATATCTCTGCTg

ShALK5
ID: TRCN0000195626
>shALK5_4 Sense
gatccGCCCTTCATTAGATCGCCCTTTCTCGAGAAAGGGCGATCTAATGAAGGGTTTTTTg
>shALK5_4 Antisense
aattcAAAAAACCCTTCATTAGATCGCCCTTTCTCGAGAAAGGGCGATCTAATGAAGGGCg

ShSmad4
ID: DPC4 UTR18
>shSmad4 Sense
ccggtAGTCCACCATCCTGATAAGGTTAAGGGTTGGCCCTTAACCTTATCAGGATGGTGGATTATTTTTTTg
>shSmad4 Antisense
aattcAAAAAAATAATCCACCATCCTGATAAGGTTAAGGGCCAACCCTTAACCTTATCAGGATGGTGGACTAc

Suppl. Figure 1 – Lonardo et al.

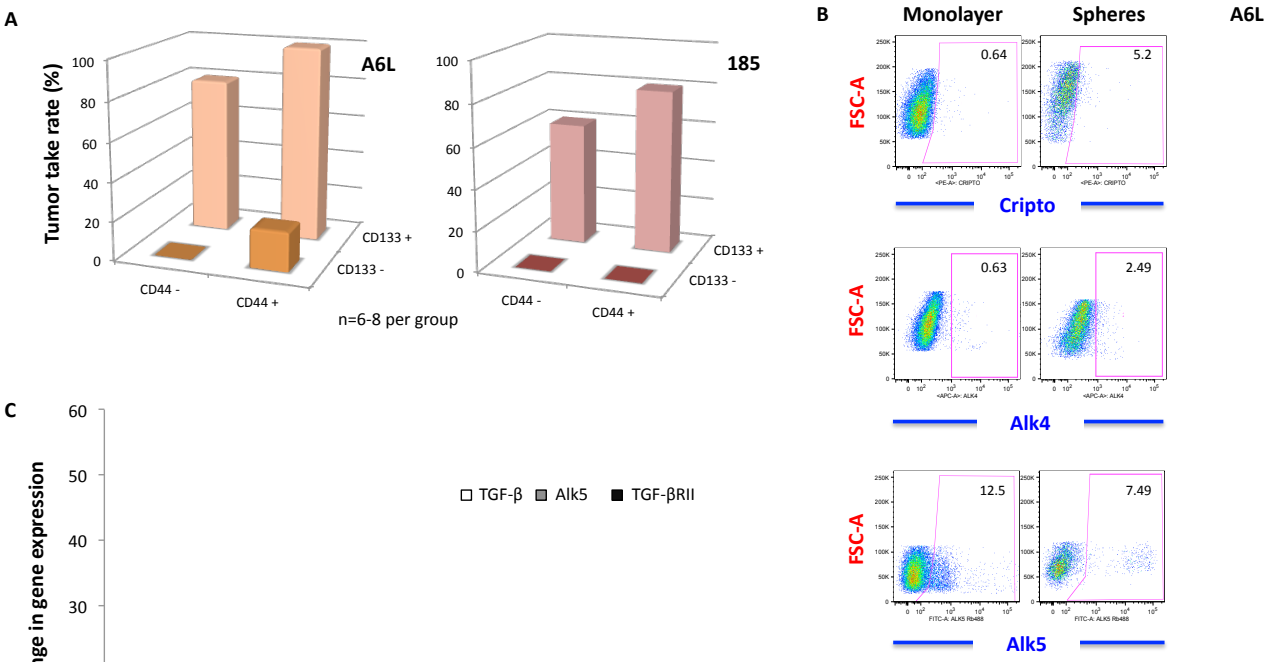

Scaling adapted to Fig. 2A; no significant differences between adherent and (s)

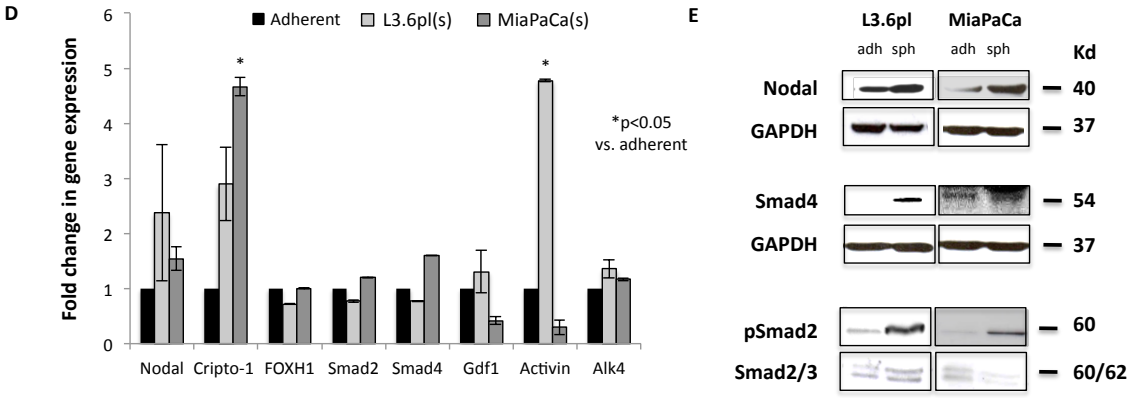

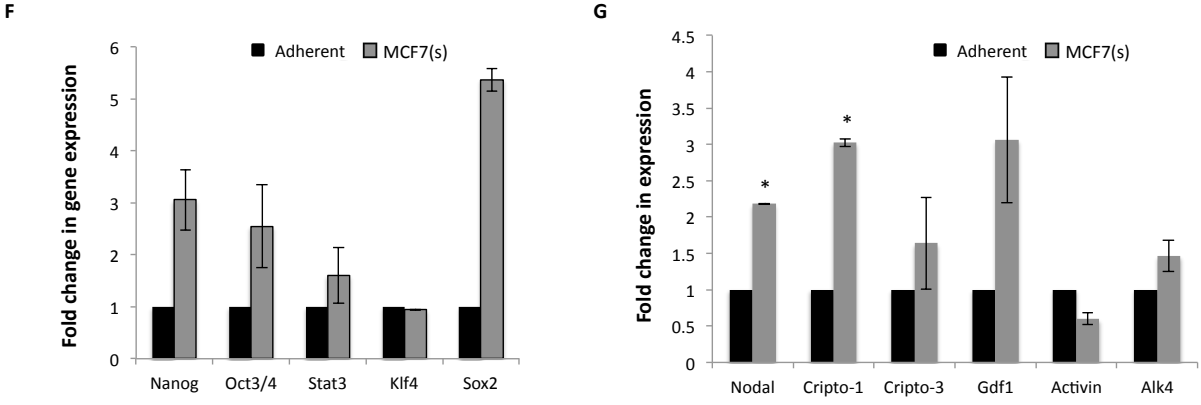

* P < 0.05

Suppl. Figure 2 – Lonardo et al.

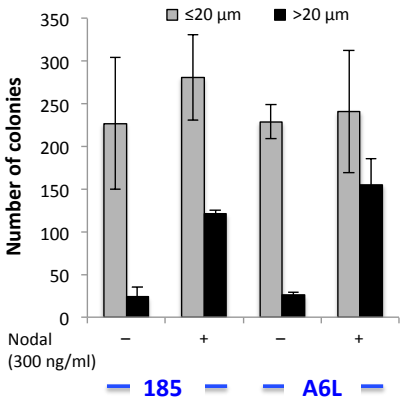

Suppl. Figure 3 – Lonardo et al.

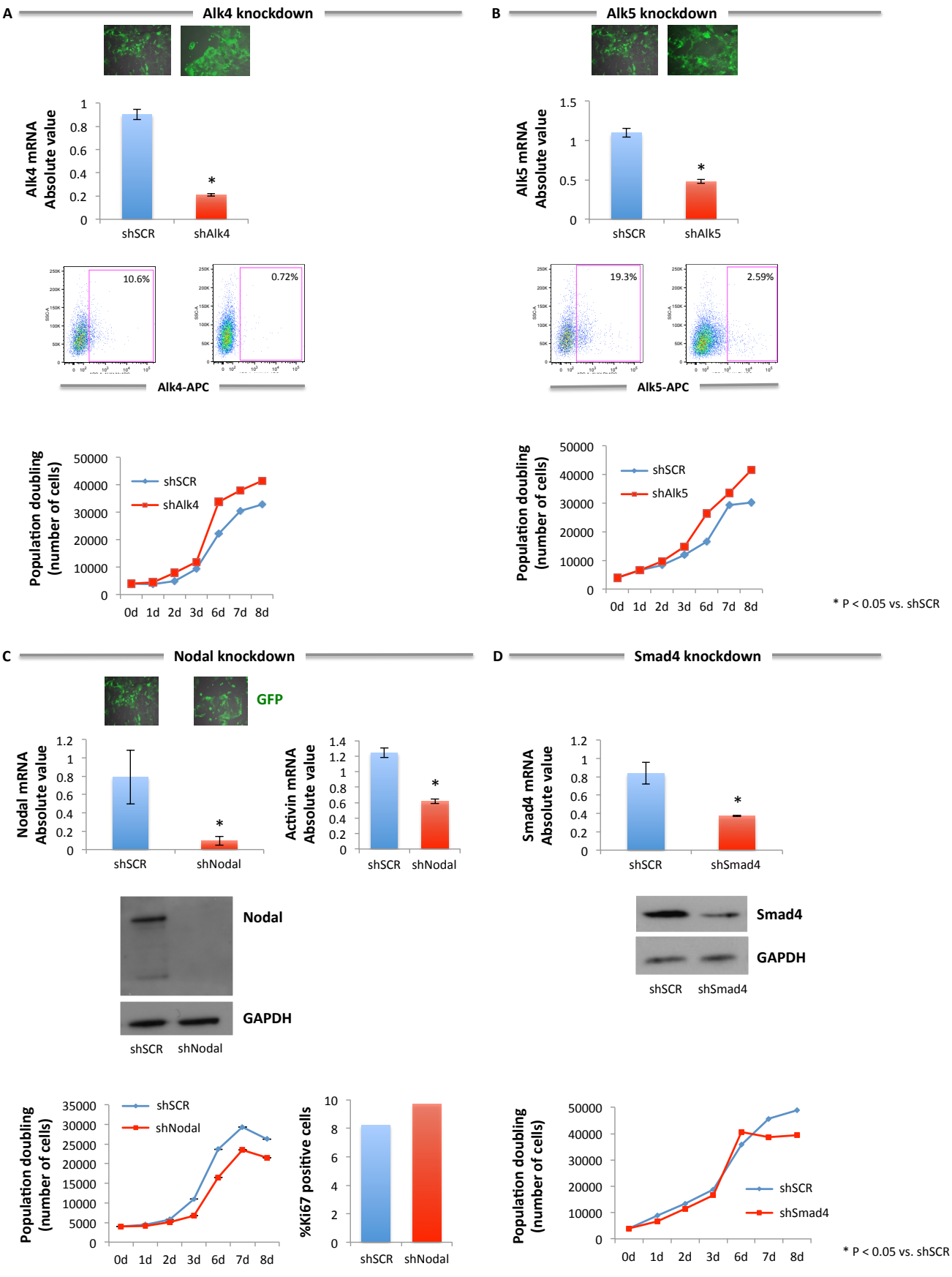

Suppl. Figure 4 – Lonardo et al.

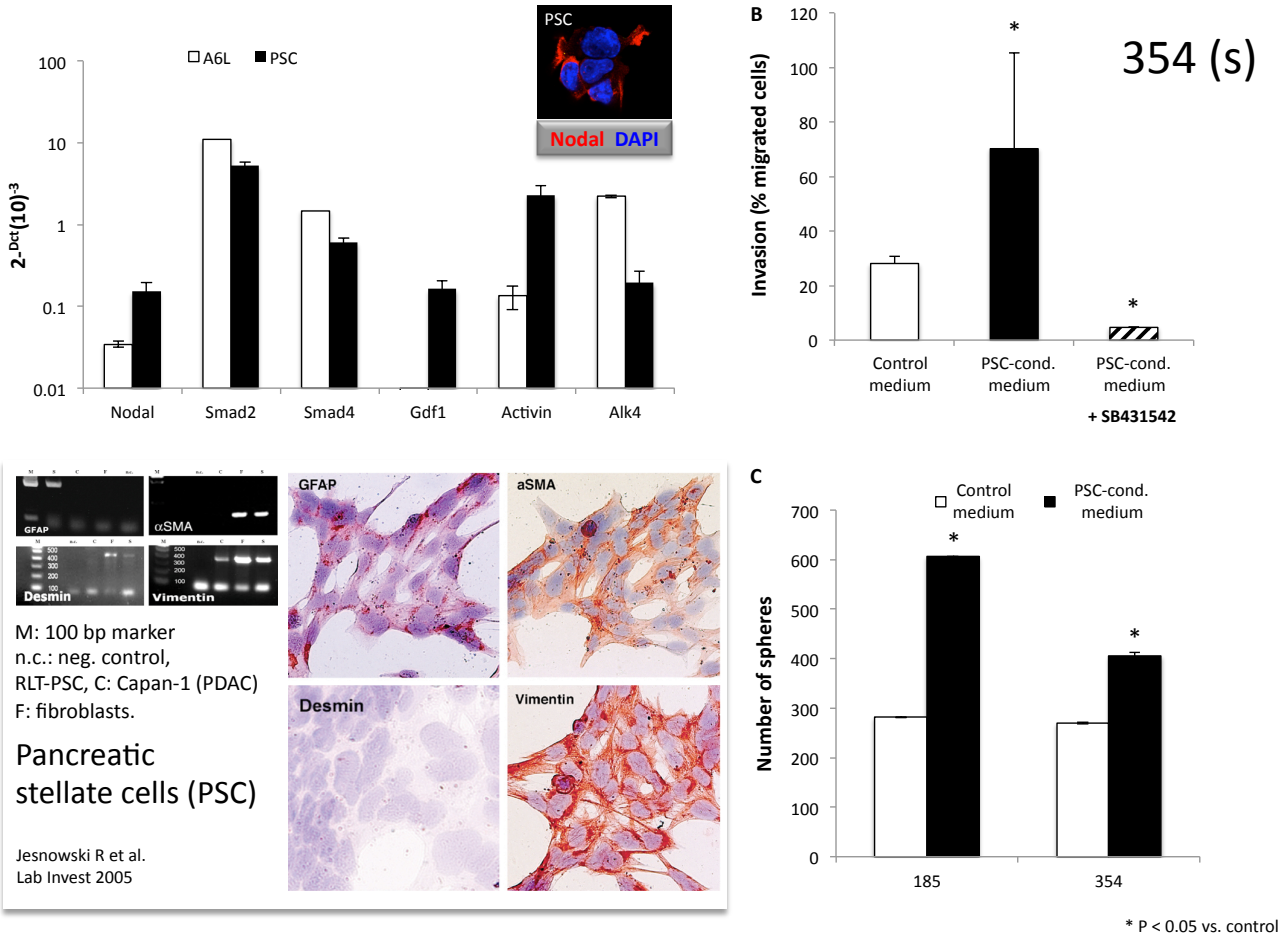

Suppl. Figure 5 – Lonardo et al.

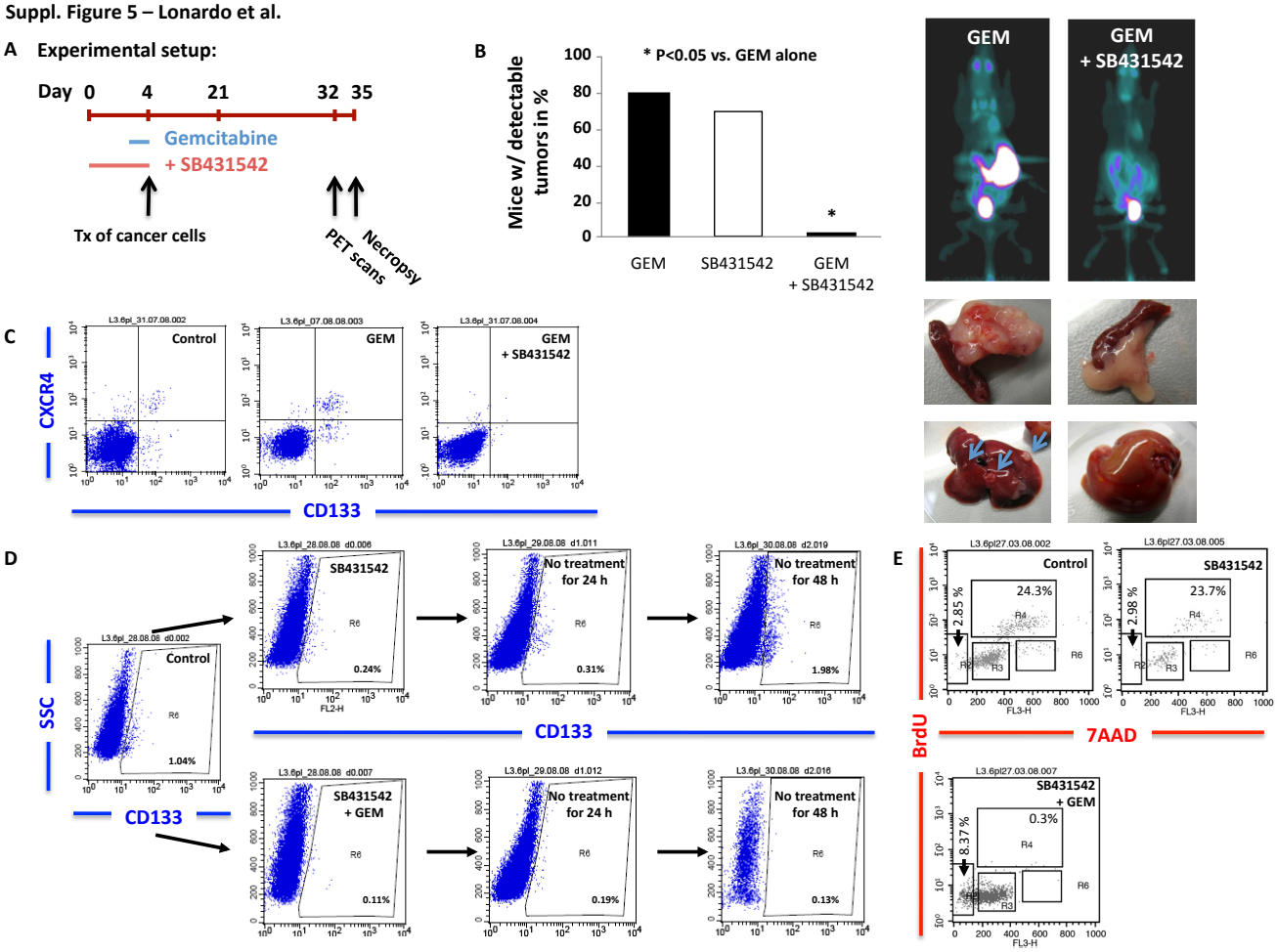

Supp. Figure 6 – Lonardo et al.

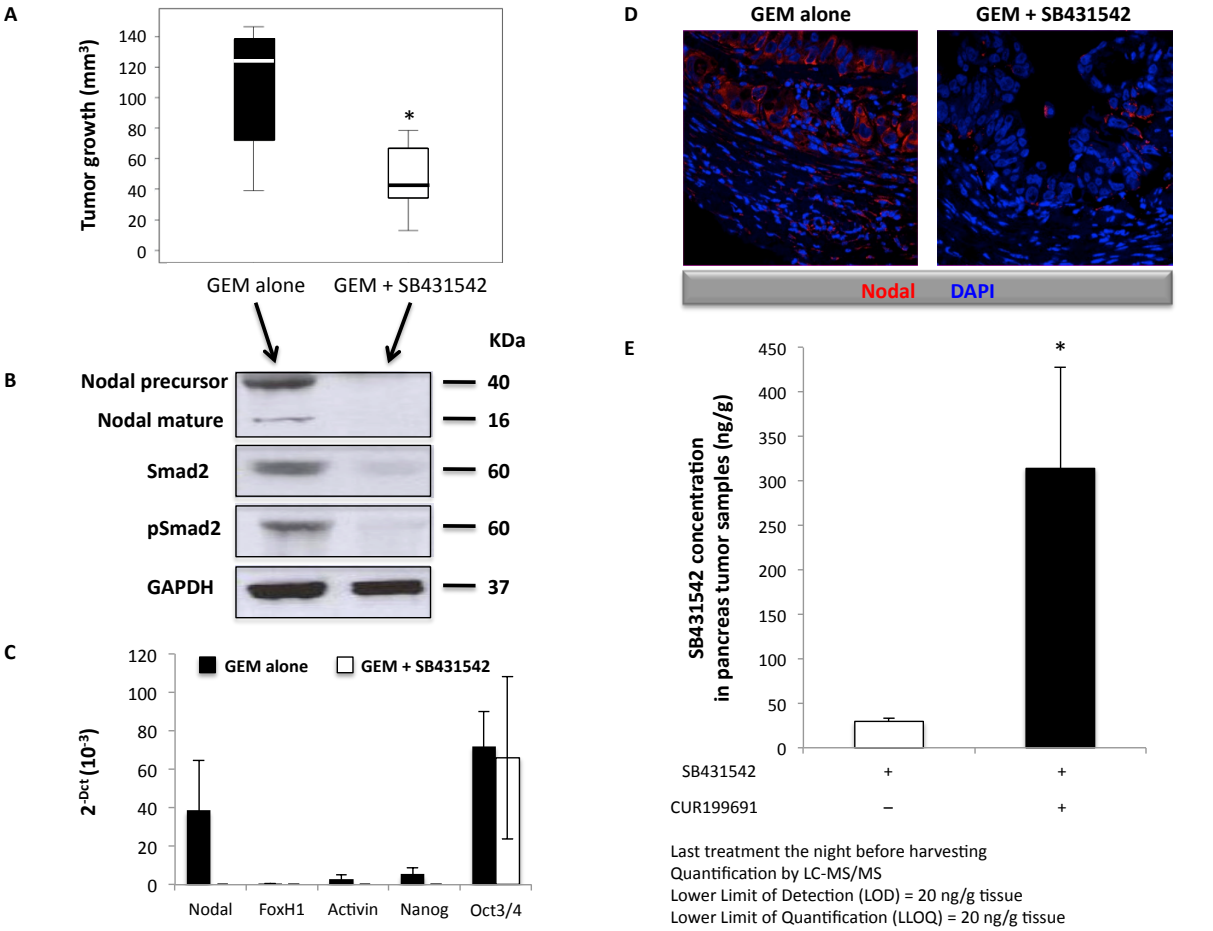

Last treatment the night before harvesting
Quantification by LC-MS/MS
Lower Limit of Detection (LOD) = 20 ng/g tissue
Lower Limit of Quantification (LLOQ) = 20 ng/g tissue

* P < 0.05 versus GEM alone

* P < 0.05 versus SB431542 alone

Suppl. Figure 7 – Lonardo et al.

A

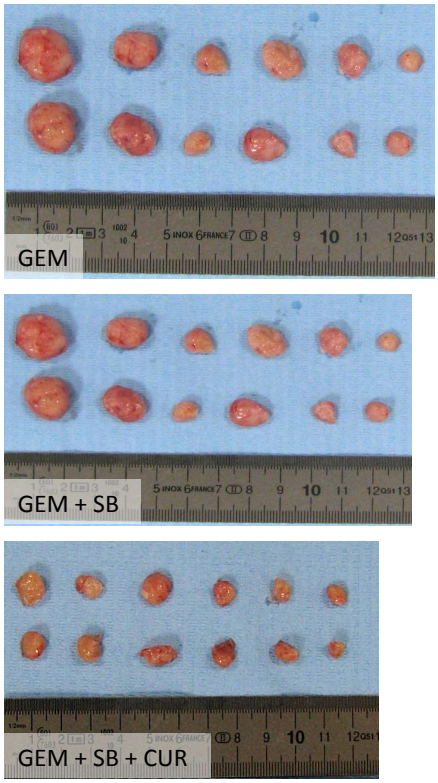

B